Conf-760724--1

LA-UR-76-1593

TITLE: THE ROLE OF ELECTRIC FIELD STRENGTH IN LASER DAMAGE OF DIELECTRIC MULTILAYERS

AUTHOR(S): Joseph H. Apfel, John S. Matteucci, Brian E. Newnam, and Dennis H. Gill

SUBMITTED TO: Symposium on Optical Materials for High Power Lasers, Boulder, Colorado, July 13-15, 1976.

0

MASTER

los alamos
scientific laboratory
of the University of California
LOS ALAMOS, NEW MEXICO 87544

An Affirmative Action/Equal Opportunity Employer

Form No. 836
St. No. 2629
1/75

UNITED STATES
ENERGY RESEARCH AND
DEVELOPMENT ADMINISTRATION
CONTRACT W-7405-ENG. 36

THE ROLE OF ELECTRIC FIELD STRENGTH IN LASER DAMAGE OF DIELECTRIC MULTILAYERS

Joseph H. Apfel and John S. Matteucci
OPTICAL COATING LABORATORY, INC.
Santa Rosa, California 95402

Brian E. Newnam and Dennis H. Gill
University of California
LOS ALAMOS SCIENTIFIC LABORATORY
Los Alamos, New Mexico 87545

The intensity of the local electric field within a multilayer illuminated by a laser beam is determined by the vector addition of forward and reverse flowing waves as a result of interference. The profile of the electric field intensity will therefore depend upon the multilayer design and can have a peak value which is more or less than the peak field of the incident beam. We have examined four multilayer designs, each composed of approximately equal numbers of high and low index films arranged so that the electric field profiles are significantly different. Laser damage thresholds for these coatings were compared with calculated electric field strength profiles.

For electron-gun evaporated titania/silica coatings damaged by 30 picosecond pulses of 1.064μm radiation the damage threshold is dictated by electric field intensity in the titania layers.

Key words: laser damage, dielectric films, electric fields, optical coatings, standing-waves

INTRODUCTION

Precision determination of laser damage thresholds is possible, yet among workers there is still uncertainty regarding the damage mechanisms. Several workers have reported experiments which support the expected relationship between damage and local electric field strength [1-3][1]. However, in multilayer coatings, the variations of material thresholds due to processing by different or common manufacturers may be masking the field strength dependence. In these studies four multilayer designs with widely different electric field enhancement factors were prepared simultaneously in one coating operation. The results of laser damage threshold experiments are then compared with calculated field strengths.

DESCRIPTION OF THE EXPERIMENTS

Figure 1 describes the multilayer designs which are composed of eight or nine layers of titanium dioxide and silicon dioxide deposited onto fused silica substrates. Design A is a simple quarter wave stack of nine layers beginning and ending with high index (TiO_2) films. In Design B the centermost layer of the quarter wave stack was omitted resulting in an eight layer design with a central, half wave optically thick, low index (SiO_2) layer. In Designs C and D the fourth or sixth layer was omitted in similar fashion.

The spectral plot of figure 1 shows that the peak transmittance of Designs B, C, and D is not precisely centered at 1.064μm. From the scan it can be inferred that the optical thicknesses of the individual layers vary by less than one percent and that both coating materials have an extinction coefficient (imaginary part of the complex refractive index) of less than 0.001.

For laser radiation incident on the coated surface of the substrate the four designs are specified as A, B, C, and D (see fig. 1). For laser radiation incident from the reverse direction, i.e. incident upon the multilayer from the substrate side, the designs are specified A', B', C', and D'. When the laser beam which is incident on the substrate at 8° passes into the fused silica it is refracted to an incident angle of 5.51°. For the reverse (primed) exposures the incidence angle onto the multilayers is therefore 5.51°.

Figure 2 and figure 3 show the computed profiles of the time averaged square of electric field strength (E^2) for each of the designs [4]. In figure 3, where radiation is incident upon the multilayer from the reverse or substrate side (primed), the incident field intensity has been adjusted to represent the same beam intensity used for the other cases (unprimed). Thus the profiles represent the field in the various designs with equal beam energy densities incident on the samples. In these figures the high and low index layers

1. Figures in brackets indicate the literature references at the end of this paper.

are distinguished by thickness. Since the optical thickness of all layers is equal, the high index layers have smaller physical thicknesses.

The coatings were prepared in a multiple spindle coating machine equipped with externally actuated masks which permit the omission of any one or more layers from substrates mounted in each spindle rack. Thus, all four designs were prepared in a single run and have minimum differences attributable to process variation.

The four 38mm diameter by 7mm thick fused silica substrates were cleaned by gentle scrubbing in a hot solution of detergent in deionized water, rinsed with deionized water and then immersed into the vapor of an alcohol dryer. Electron beam heated evaporation sources with copper rotary hearths were used for deposition. The titanium dioxide films were deposited at 80Å/min. and the silicon dioxide at 175Å/min. onto substrates held at 225°C.

The completed coatings were exposed to 30ps pulses of 1.064μm radiation as described previously [1]. Each sample was tested with radiation polarized in the *s* plane and incident on the coated side of the substrate, and from the reverse direction, at an angle of 8°.

RESULTS

Table I and figure 4 include the measured laser damage threshold ranges. The top end of the threshold range was defined as the maximum pulse energy density for which neither visible damage nor spark radiation of a minimum value was detected. The lower end was defined as the minimum pulse energy density for which damage was detected either by the LIS method or by the occurrence of a spark with at least the prescribed radiant energy. An average of 68 laser shots were made for each range determination; the number for each is shown in figure 4.

TABLE I

DAMAGE THRESHOLDS OF TiO_2/SiO_2 MULTILAYER DESIGNS
Pulse Energy Density - J/cm²

DESIGN	INCIDENT FROM AIR	INCIDENT FROM SUBSTRATE*
A	4.8 - 7.4	3.6 - 4.4
B	3.5 - 4.5	2.9 - 3.3
C	4.4 - 5.6	1.55 - 1.85
D	1.46 - 1.68	2.1 - 2.8

*Pulse energy densities incident upon the multilayer from within the fused silica substrate.

DISCUSSION OF RESULTS

We have attempted to fit the experimental threshold range determinations to computed values for three models of electric field dependence. It is assumed that the damage will correlate with field strength in either the high (TiO_2) or low (SiO_2) index layers.

Model 1 assumes that damage occurs in either material when the local field exceeds a threshold value. This is the simplest model, and probably the most applicable. If damage results from homogeneous absorption or from pure avalanche breakdown, this model should apply. The predicted thresholds for the two materials in the eight configurations will be proportional to the reciprocals of the peak E^2 values (see figs. 2, 3, and 5). Figure 6 (Model 1) shows the result of a least squares fit[2] of the mean value of the experimental ranges to the predicted thresholds for both high (TiO_2) and low (SiO_2) index failure.

High index failure is the best fit as indicated by a standard deviation[3] of 0.43 compared to the next lowest value of 0.60 for Model 2 (see below). The slope of the best fit line for high index failure corresponds to an RMS electric field of 7.9MV/cm.

In Model 2 it is assumed that damage occurs when the volume integral of the time average squared field over one layer equals the threshold value. This integral is proportional to the area on the E^2 plots (see figs. 2, 3, and 5). The model would apply if damage results when the total homogeneous absorption in a layer reaches threshold value. Since the layers have equal thickness, the value of the integral is proportional to the average value of E^2. Figure 7 is a plot of the least squares fit of experimental data to Model 2. High index failure is again a better fit with the data.

Model 3 is similar to Model 2 except that the total integral of E^2 is taken over all layers of the same material throughout the multilayer. The fit between experiment and model shown in figure 8 is not very good.

Failure due to peak electric field in the high index layers is indicated by these results. The fact that Model 2 is close to Model 1 is consistent with the shape of the profiles (see figs. 2, 3, and 5) because the area under each layer profile is approximately proportional to the peak height of the profile.

Sample B (Designs B and B') are critical to the separation of failure due to high or low index materials. In the other three samples the peak fields are equal for both materials so the experiments will not distinguish which fails. Only when data from Sample B are included can we distinguish the materials.

2. The least squares fit was made by minimizing the square of the deviations of the mean threshold values from a straight line through the origin.

3. The standard deviation is here defined as the square root of the mean

Figure 9 shows the electric field profiles for the eight designs with incident intensities adjusted to equal the upper and lower ends of the experimental threshold ranges. On each profile small horizontal lines have been added to indicate the best fit solution of Model 1. These lines correspond to an internal RMS electric field of 7.9MV/cm.

If we assume that thresholds are correlated with the peak electric field in the high index (TiO_2) layers, then it is interesting to speculate about the discrepencies in the fit of Model 1. The fit is improved if the threshold data from Sample A are omitted. Table II shows how the peak field locations are distributed throughout various designs. Notice that Sample A (Designs A and A') have peak fields in the outermost and innermost layers whereas Samples B, C, and D have peaks confined to the four central layers.

TABLE II

IDENTIFICATION OF LAYER IN WHICH THE PEAK ELECTRIC FIELD OCCURS FOR BOTH MATERIALS

	Designs							
Layer*	A	B	C	D	A'	B'	C'	D'
1	H				H			
2	L		L		L		L	
3	H	H	H			H	H	
4	L	L	O	L		L	O	L
5	H	O	H	H		O	H	H
6	L	L	L	O		L	L	O
7	H	H		H		H		H
8	L	L		L				L
9	H	H						

*count layers from substrate

O indicates an omitted layer

On the assumption that the outer and innermost pairs of layers may have different thresholds than the others, Model 1' is presented (see fig. 10). Here the experimental threshold ranges are fit only to Samples B, C, and D. The comparable data for Designs A and A' are shown but they were not used in determining the least squares fit. The standard deviation, calculated for the six data points, is 0.24 for the high index failure and shows improvement compared to 0.43 for Model 1. The slope of the best fit line for high index failure in Model 1' corresponds to an RMS electric field of 8.3MV/cm.

In Model 1' (fig. 10) the experimental threshold is below the predicted value for high index failure in Design A'. Perhaps this indicates that the first layer adjacent to the substrate is induced to lower threshold by a phenomenon not considered in this analysis. A simple explanation of this discrepancy is not likely to also cover the case of Design B' in which the threshold range is slightly higher than prediction.

The peak fields in the low index (SiO_2) layers numbered 4 and 6 of Sample B are very high when damage occurs. According to the computation, the peak time average square of field in the low index layers is 2.3 times the peak in the high index layers, therefore, the central low index layers of Sample B are experiencing an RMS field of 12MV/cm at the threshold of damage.

In their damage studies of sputtered single TiO_2 layers, Gill, Newnam, Hartman, and Coleman [5] found a threshold range of 8-11.3 Joules/cm^2 for 30ps pulses. The RMS field within the film, computed from an electric field profile, was 6.9 to 8.3MV/cm. Smith, Bechtel, and Bloembergen [6] found an RMS breakdown field strength of 11.7MV/cm for fused silica window material.

CONCLUSIONS

We have investigated the laser damage threshold for several multilayer designs produced under identical conditions. The results indicate that the peak pulse energy density at threshold produces an RMS electric field about 8MV/cm in the high index titanium dioxide layers of each design. This compares with the field in the most damage resistant films previously reported. The field in the low index silicon dioxide layers varies between 8 and 12 MV/cm and is felt not to induce failure.

There is an indication that the first high index layer coated on the fused silica substrate may have a lowered threshold. This could be due to coating process variation or to substrate induced defects.

FIG. 1. Schematic description and spectral transmittance plots of the four multilayer designs.

FIG. 2. Electric field profiles for the four designs for s plane radiation incident at 8° from the air side. The abscissa is physical thickness measured normal to the layers and the ordinate is the computed value of the time average of the square of the electric field. Each profile is shown for an optical half wave distance in the incident medium and for a short distance into the substrate where there is no standing wave. The field intensity of the incident beam is indicated by the arrow on each plot. The dotted lines connect the location of omitted layers with Sample A.

FIG. 3. Similar to figure 2 except the radiation is incident on each design at 5.51° from the substrate side. The incident field intensity has been adjusted for first surface reflection and for substrate refractive index so that profiles can be compared with figure 2 for equal laser pulse energy density.

FIG. 4. Experimental laser damage thresholds for the four multilayer designs. Data from Table I for the samples irradiated from substrate side (primed) have been corrected for first surface reflection loss before inclusion in this plot. The number of laser shots is given for each test.

FIG. 5. Graphical description of the models used for prediction of damage thresholds attributable to high index layers. Model 1 uses the peak value, Model 2 used the peak volume integral represented by indicated shading, and Model 3 uses the total volume integral of E^2.

FIG. 6. Model 1. Best fit of experimental results to prediction if threshold is proportional to the reciprocal of the peak $\overline{E^2}$ in the multilayers. The numbers are the standard deviations of the plotted lines relative to the mean values of the threshold ranges.

FIG. 7. Model 2. Best fit of experimental results to prediction if threshold is proportional to the reciprocal of the maximum integrated time averaged square of electric field over one layer. The numbers are the standard deviations of the plotted lines relative to the mean values of the threshold ranges.

FIG. 8. Model 3. Best fit of experimental results to prediction if threshold is proportional to the reciprocal of the sum over all layers of similar index of the integrated time averaged square of the electric field. The numbers are the standard deviations of the plotted lines relative to the mean values of the threshold ranges.

FIG. 9. Electric field profiles for the four designs with incident intensities adjusted to equal the extremes of observed laser damage ranges for radiation incident from air side and from substrate side (primed). The short horizontal lines indicate the RMS field of 7.9MV/cm.

FIG. 10. Model 1'. Best fit of experimental results to prediction if threshold is proportional to the reciprocal of the peak $\hat{E}^2$ in the multilayers. Only Samples B, C, and D were used in establishing the best fit, otherwise this is similar to Model 1.

REFERENCES

1. B. E. Newnam, D. H. Gill, and G. Faulkner, "Influence of Standing Wave Fields on the Laser Damage Resistance of Dielectric Films", NBS Special Publication No. 435, 254 (1975).

2. N. L. Boling, M. D. Crisp, and G. Dubé, "Laser Induced Surface Damage", Appl. Opt. 12, 650 (1973).

3. B. E. Newnam and D. H. Gill, "Laser Damage Resistance and Standing-Wave Fields in Dielectric Coatings", J. Opt. Soc. Am. 66, 166 (1976).

4. J. H. Apfel, "Electric Fields in Multilayers at Oblique Incidence", to be published in Applied Optics, October 1976.

5. D. H. Gill, B. E. Newnam, J. S. Hartman, and W. J. Coleman, "Super-High Damage Thresholds for RF-Sputtered TiO_2 Films", J. Opt. Soc. Am. 66, 78 (1976).

6. W. L. Smith, J. H. Bechtel, and N. Bloembergen, "Picosecond Breakdown Studies", NBS Special Publication No. 435, 321, (1975).

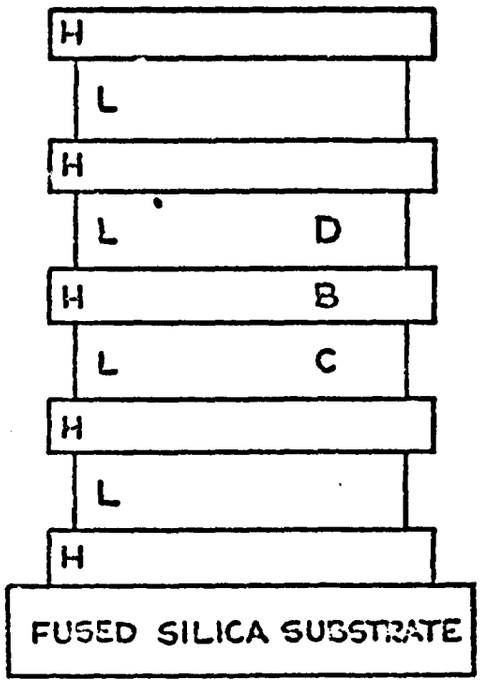

DESIGN A, A NINE LAYER QUARTER WAVE STACK FROM WHICH IDENTIFIED LAYERS WERE OMITTED TO FORM DESIGNS B, C, AND D.

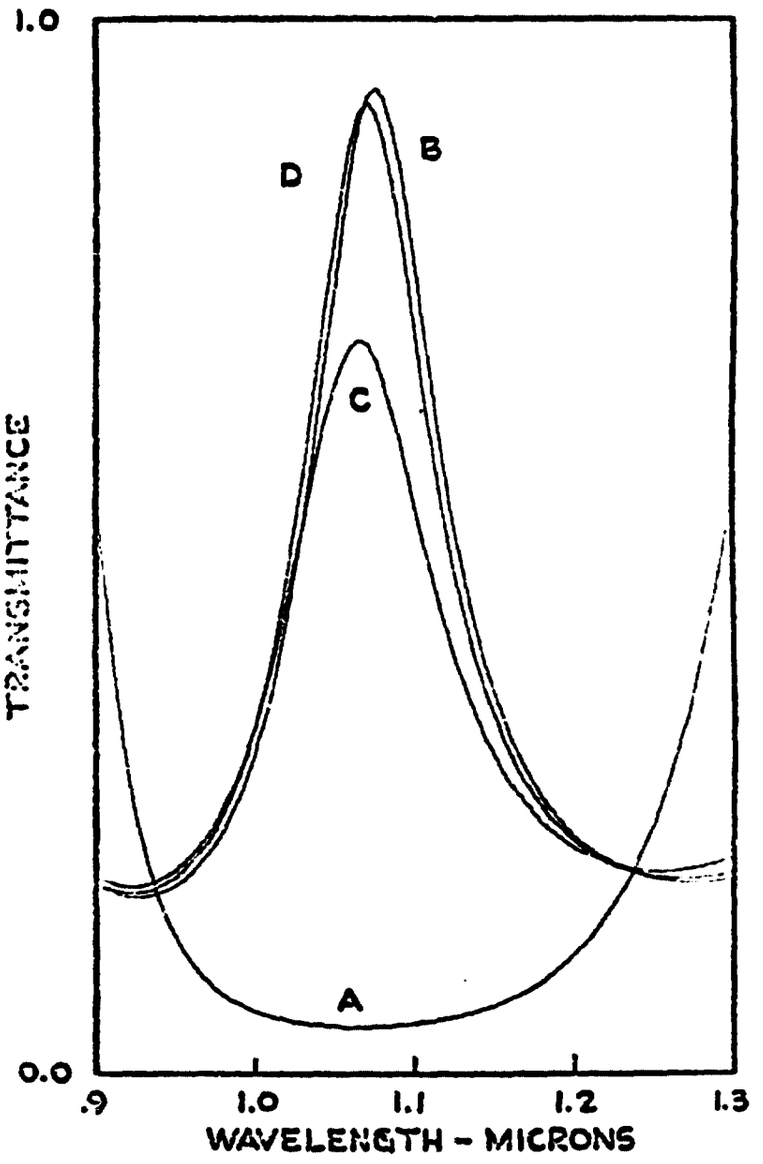

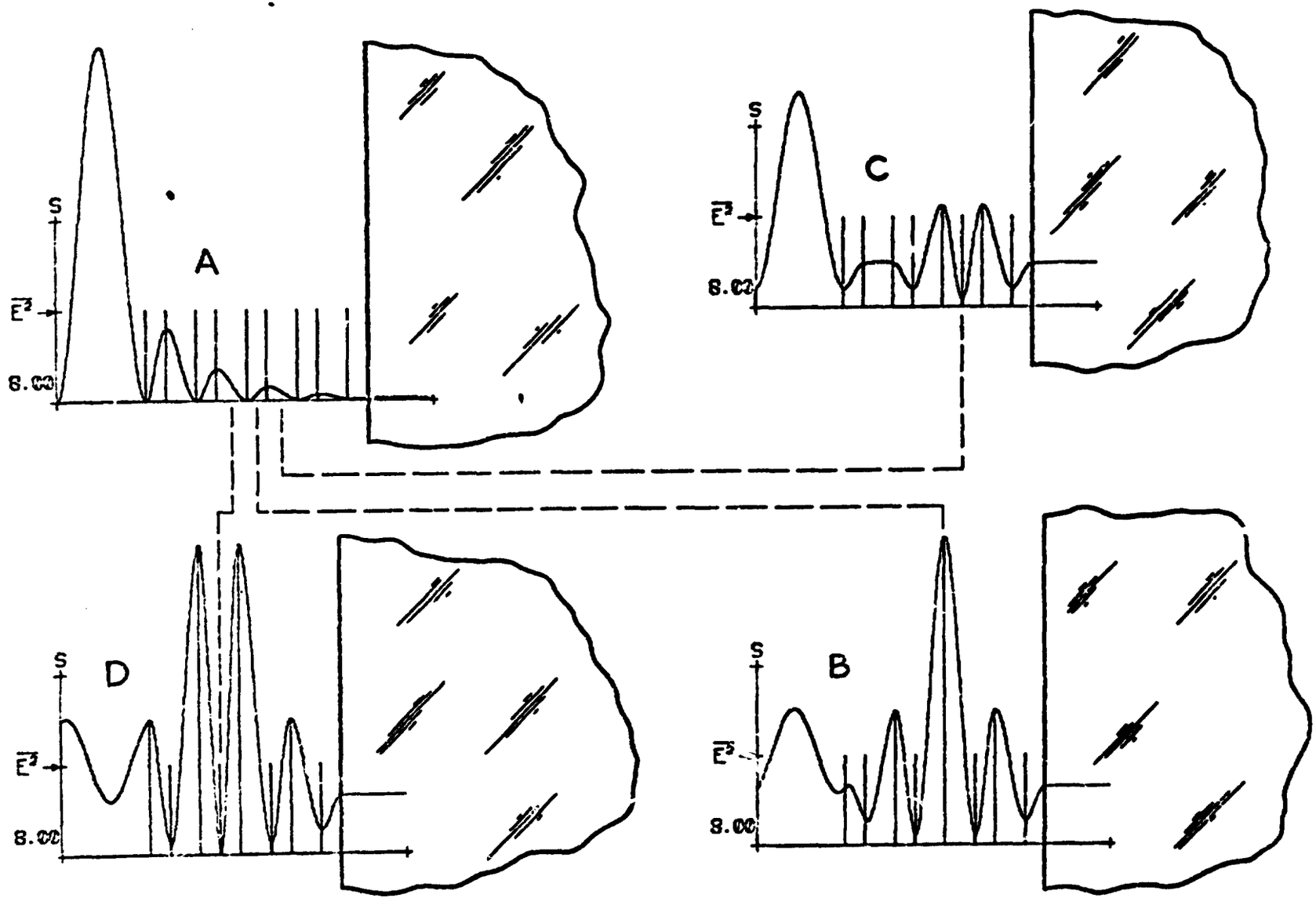
A
S
$\overline{E^2}$
8.00
C
S
$\overline{E^2}$
8.00
D
S
$\overline{E^2}$
8.00
B
S
$\overline{E^2}$
8.00

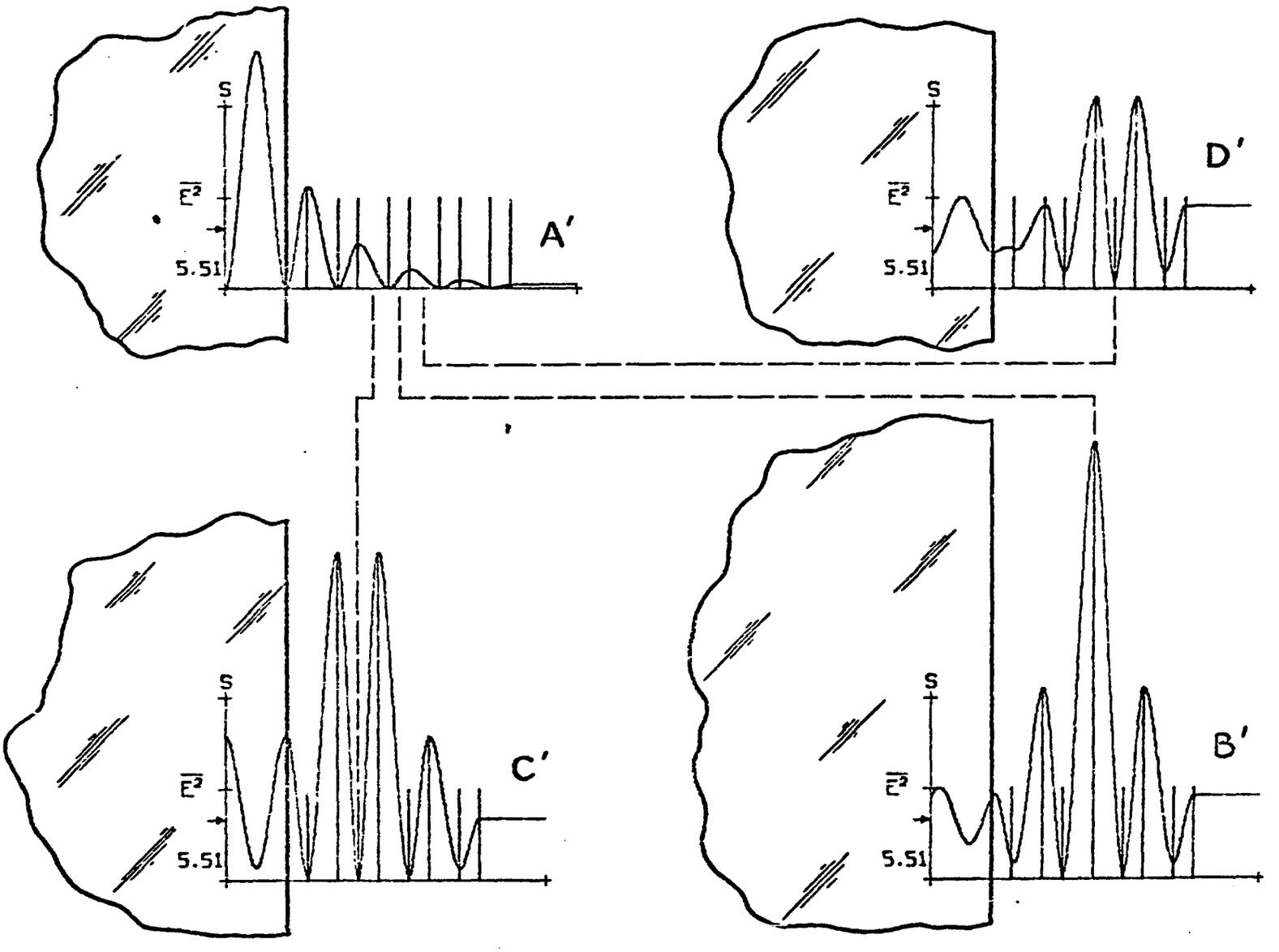
S
$\overline{E^2}$
5.51
A'
D'
C'
B'

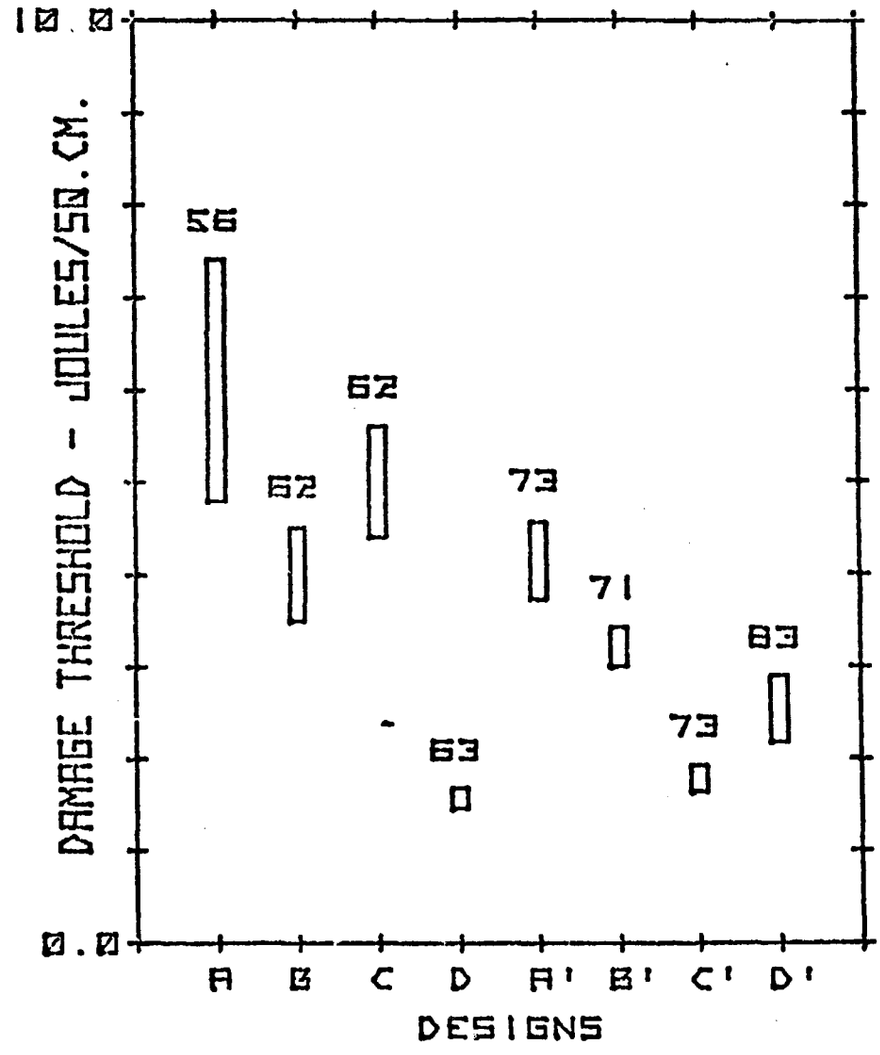
10.0
0.0
DAMAGE THRESHOLD - JOULES/SQ.CM.
56
62
62
63
73
71
73
83
A
B
C
D
A'
B'
C'
D'
DESIGNS

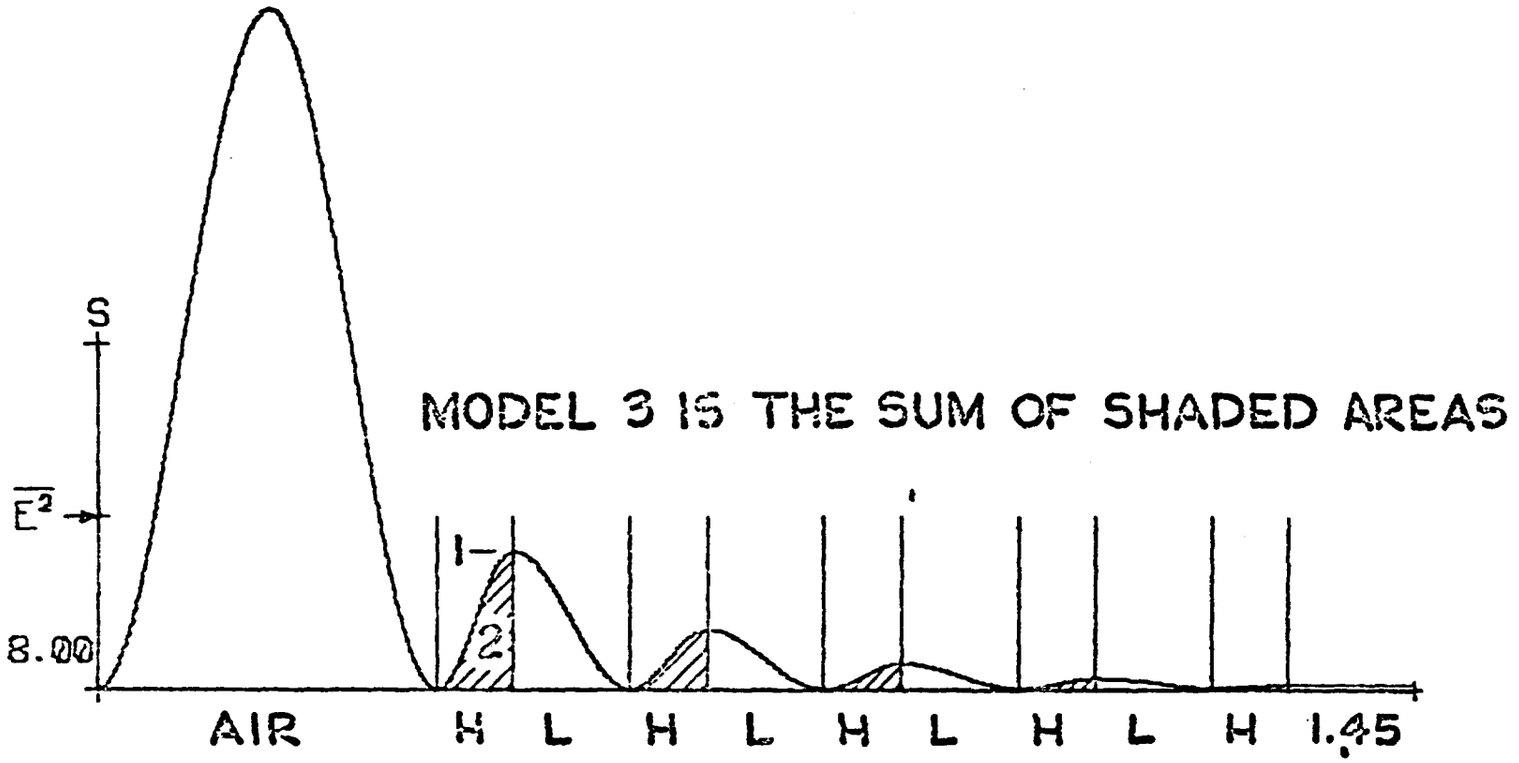
MODEL 3 IS THE SUM OF SHADED AREAS
S
$\overline{E^2}$
8.00
1
2
AIR
H
L
H
L
H
L
H
L
H
1.45

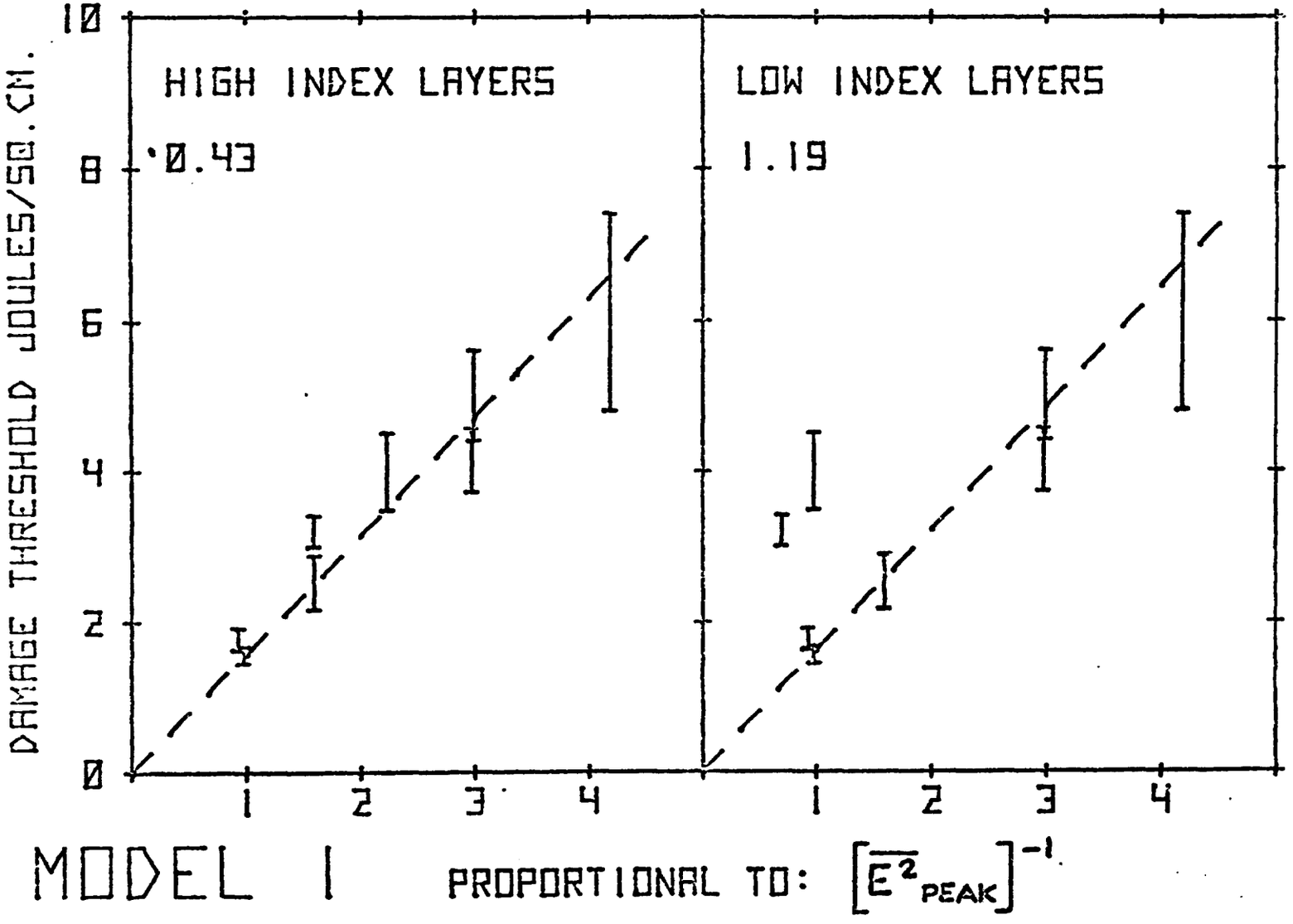
HIGH INDEX LAYERS
0.43
LOW INDEX LAYERS
1.19
DAMAGE THRESHOLD JOULES/SQ.CM.
0
2
4
6
8
10
1
2
3
4
MODEL I
PROPORTIONAL TO: $[\overline{E^2}_{PEAK}]^{-1}$

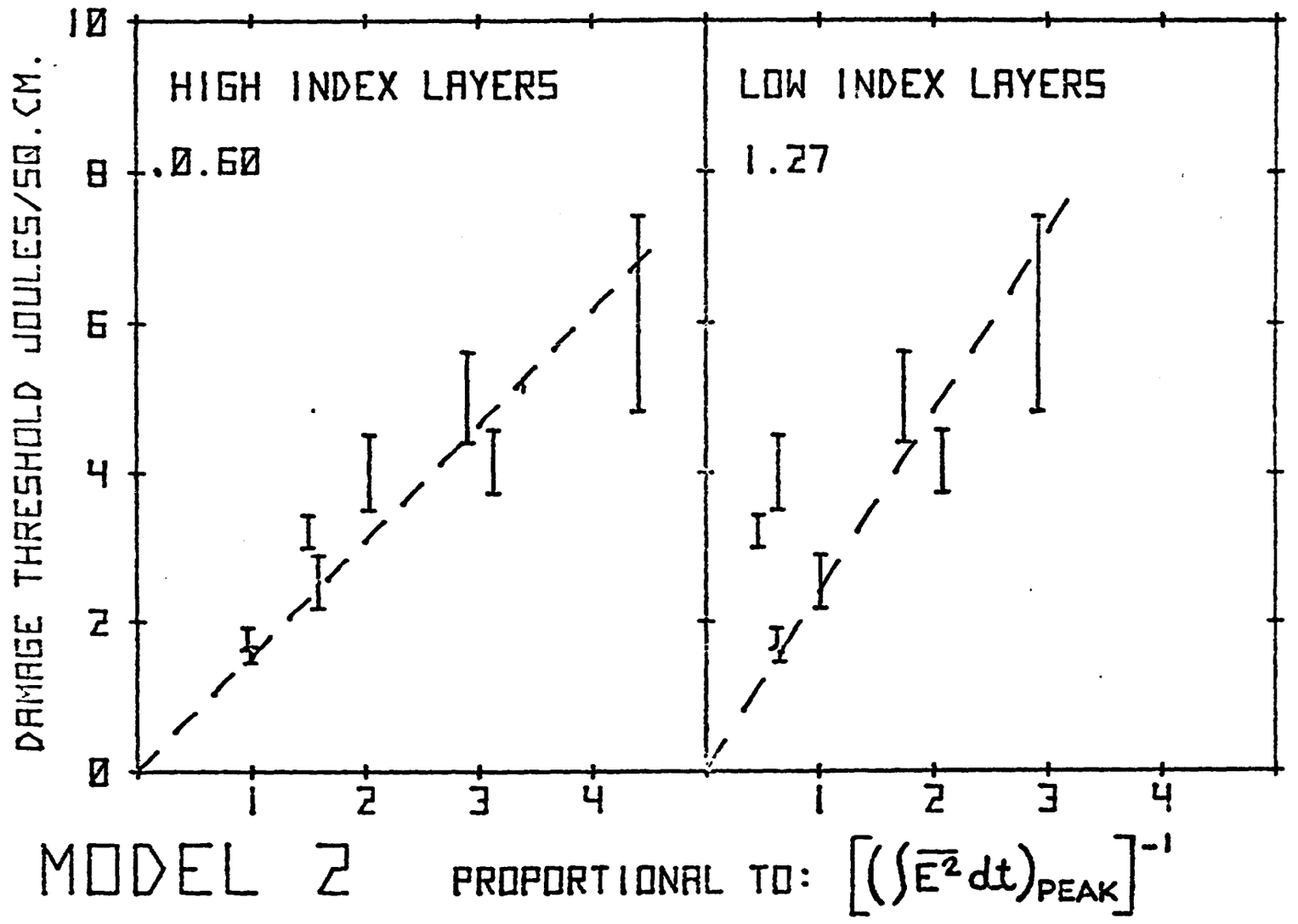
HIGH INDEX LAYERS
.0.60
LOW INDEX LAYERS
1.27
DAMAGE THRESHOLD JOULES/SQ.CM.
10
8
6
4
2
0
1
2
3
4
1
2
3
4
MODEL 2
PROPORTIONAL TO: $\left[\left(\int \overline{E^2}\, dt\right)_{PEAK}\right]^{-1}$

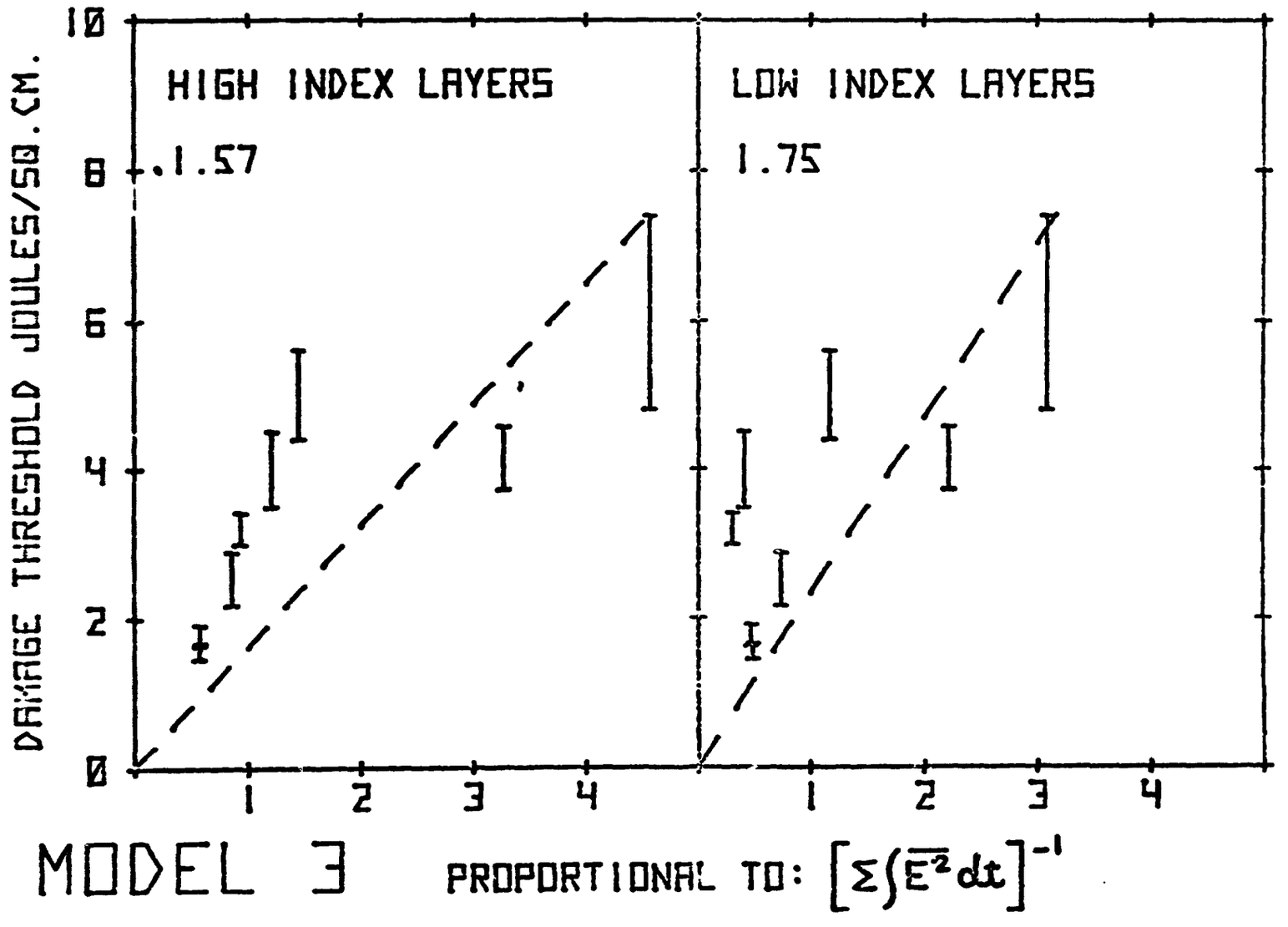
HIGH INDEX LAYERS
1.57
LOW INDEX LAYERS
1.75
DAMAGE THRESHOLD JOULES/SQ.CM.
0
2
4
6
8
10
1
2
3
4
MODEL 3
PROPORTIONAL TO: $[\Sigma \int \bar{E}^2 dt]^{-1}$

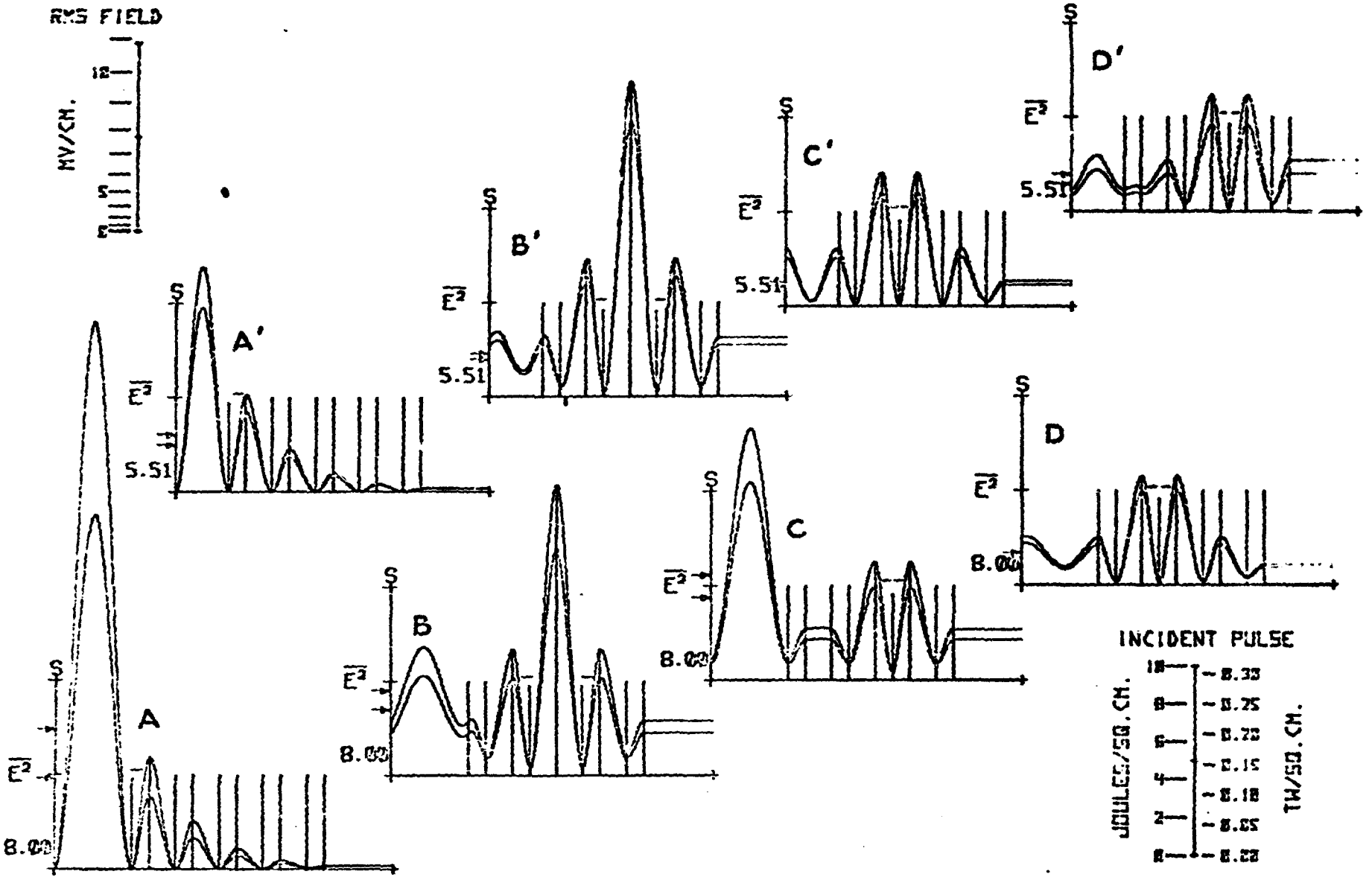
RMS FIELD
MV/CM.
INCIDENT PULSE
JOULES/50.CM.
TW/50.CM.
A
A'
B
B'
C
C'
D
D'
S
$\overline{E^2}$
5.51
8.00

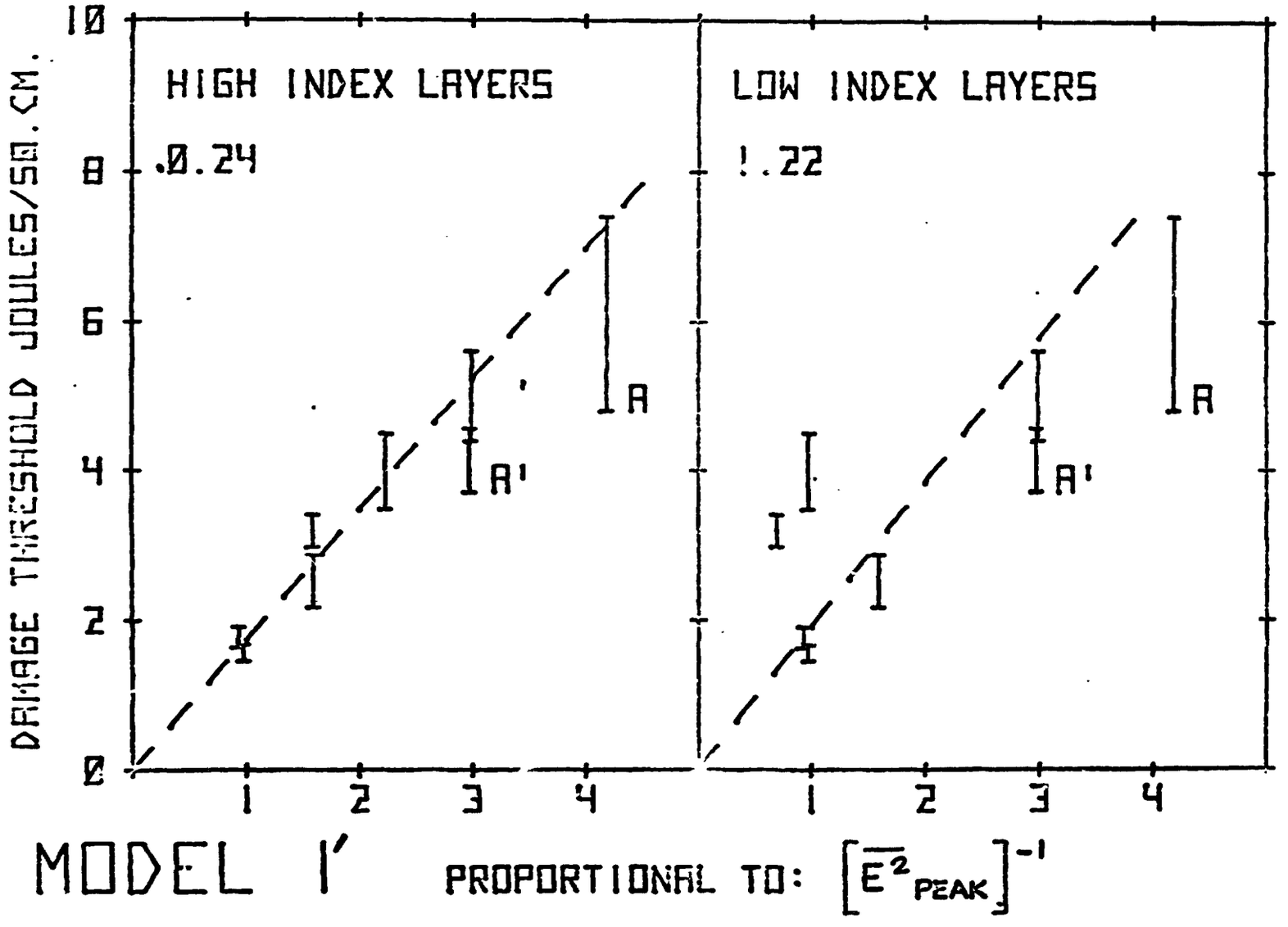
DAMAGE THRESHOLD JOULES/SQ.CM.
10
8
6
4
2
0
HIGH INDEX LAYERS
.0.24
LOW INDEX LAYERS
!.22
A
A'
A
A'
1
2
3
4
1
2
3
4
MODEL 1'
PROPORTIONAL TO: $[\overline{E^2}_{PEAK}]^{-1}$